Journal of Asian Earth Sciences 44 (2012) 169–175

Contents lists available at SciVerse ScienceDirect

Journal of Asian Earth Sciences

journal homepage: www.elsevier.com/locate/jseaes

Magnetostratigraphy of the Suerkuli Basin indicates Pliocene (3.2 Ma) activity of the middle Altyn Tagh Fault, northern Tibetan Plateau

Hong Chang [a,*], Hong Ao [a], Zhisheng An [a], Xiaomin Fang [b], Yougui Song [a], Xiaoke Qiang [a]

[a] State Key Laboratory of Loess and Quaternary Geology, Institute of Earth Environment, Chinese Academy of Sciences, Xian 710075, China
[b] Institute of Tibetan Plateau Research, Chinese Academy of Sciences, Beijing 100085, China

ARTICLE INFO

Article history:
Available online 25 November 2011

Keywords:
Magnetostratigraphy
Altyn Tagh Fault
Tectonic uplift
Suerkuli Basin
Pliocene

ABSTRACT

The left-lateral strike-slip Altyn Tagh Fault (ATF) forming the northern boundary of the Tibetan Plateau accommodates parts of the overall convergence between the colliding Indian and Eurasian plates. Precise dating of the ATF activity is essential for understanding possible mechanisms of Tibetan Plateau deformation and uplift. Here we report a magnetostratigraphic study of the Suerkuli Basin deposits recording depositional changes during the ATF activity. Field investigations reveal a remarkable and widespread change in depositional environment in the Suerkuli Basin, i.e. a transformation from low-energy lacustrine deposits (grayish-green mud-siltstone and brown mud-siltstone) into high-energy alluvial fan deposits (poorly sorted gray pebble and cobble conglomerates). Detailed magnetostratigraphy of the 390-m-thick Daban section, at the southeastern margin of the Suerkuli Basin (38°43.09′N, 90°58.84′E), shows that this change in depositional facies occurred at ~3.2 Ma, accompanied by a remarkable increase in sediment accumulation rate. We attribute this depositional change to the Piocene tectonic activity of the middle ATF although the contribution of the Pliocene global climate deterioration cannot be excluded.

1. Introduction

The Altyn Tagh Fault (ATF) is the geologic boundary between the Tibetan Plateau and the Tarim Basin in northwest China. As such it is one of the major geomorphologic boundaries on Earth and marks the abrupt transition from the world's highest plateau to the world's second largest desert basin. As a left-lateral and strike-slip fault, the ATF accommodates a large part of the overall convergence between the Indian and Eurasian plates (Avouac and Tapponnier, 1993; Dupont-Nivet et al., 2004; Zhang et al., 2004). It provides an ideal setting to understand uplift, erosion and sedimentation processes and their relations to lithospheric deformation and global or regional climate changes linked to the Indo-Asia collision and Tibetan Plateau uplift dynamics. Thus precise dating of the ATF activity is crucial for understanding the possible mechanisms of Tibetan Plateau uplift and its effects on climate changes.

The ATF has a protracted history starting probably in the early Cenozoic and continuing in response to the northward propagation of deformation related to the India-Eurasia continental collision along with the uplift of the Tibetan Plateau (Yin et al., 2002; Yue et al., 2003). It is presently active and uplifted to its present elevation of ca. 4000 meters above sea level (Washburn et al., 2004). A set of Cenozoic basins formed adjacent to the ATF recording the precise history of the fault activity (e.g. Dupont-Nivet and Butler, 2003; Sun et al., 2005a,b; Yue et al., 2003). However, the depositional age in most of these basins is still poorly constrained although they are potentially suitable for magnetostratigraphic dating. In the present study, we report a magnetostratigraphic dating of a set of sediments from the Suerkuli Basin along the central segment of the ATF, which has potential implications for ATF activity in the late Cenozoic.

2. Geological setting and sampling

The Suerkuli Basin (Fig. 1) is described as a strike-slip fault related basin (Li et al., 2002), belonging to the Qaidam Basin before the ATF activation (Yin et al., 2002; Meng et al., 2003). Due to the ATF activity and associated uplift, it now reaches an elevation of ~3500 m. The stratigraphic sequence in the basin reveals a remarkably widespread change in depositional environment characterized by transformation of low-energy lacustrine deposits (grayish-green mud-siltstone and brown mud-siltstone) into high-energy alluvium fan deposits (poorly sorted gray pebble and cobble conglomerates).

The studied site is located at Daban (38°43.09′N, 90°58.84′E), which lies at the southeastern margin of the Suerkuli Basin (Fig. 1b). Here the Pliocene sediment has a thickness of ~390 m, which is named as the Shizigou Formation (Li and Zheng, 1982).

* Corresponding author. Tel.: +86 29 88321470.
E-mail address: changh@loess.llqg.ac.cn (H. Chang).

1367-9120/$ - see front matter © 2011 Elsevier Ltd. All rights reserved.
doi:10.1016/j.jseaes.2011.10.013

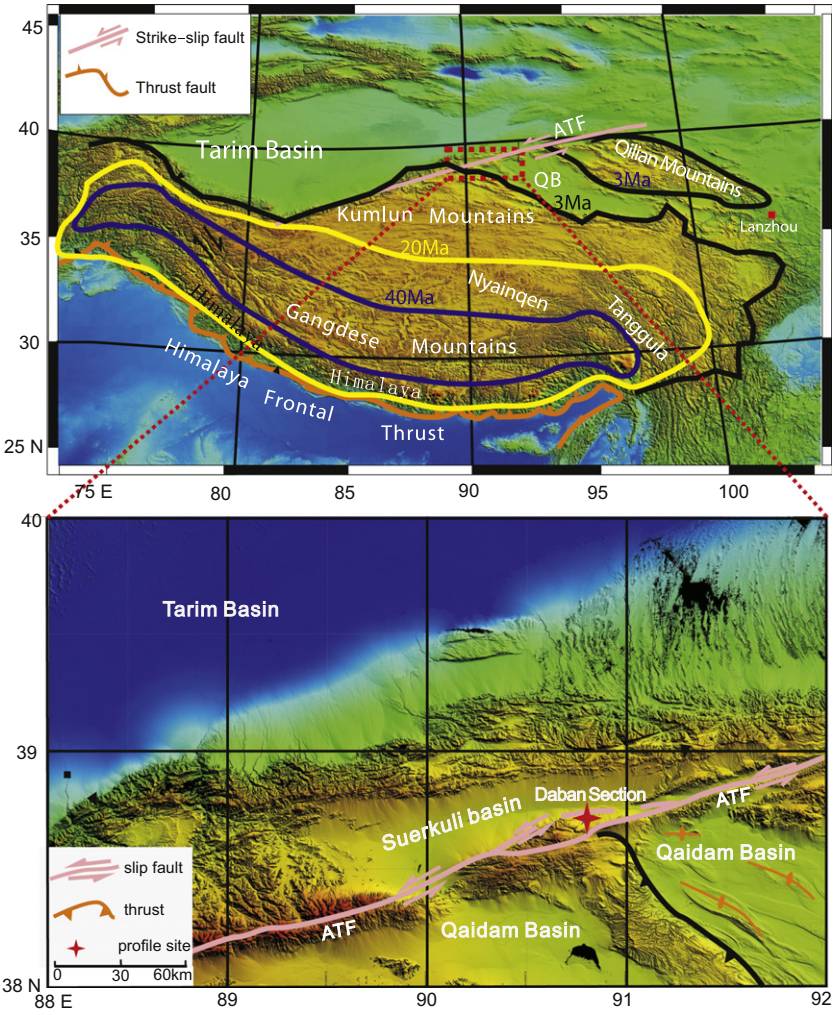

Fig. 1. Location map of the Suerkuli Basin and Daban section on digital elevation model of the Tibetan Plateau with modeled evolution of the topography from Rowley and Currie (2006). ATF: Altyn Tagh Fault, QB: Qaidam Basin.

It can be divided into two parts according to lithology (Fig. 2a). The lower part has a thickness of ~320 m, consisting of fine-grained grayish-green mud-siltstone and brown mud-siltstone with associated gypsum and gray conglomerate layers, in which some Pliocene fossils (such as *Obtusochara* sp. and *Charies* sp.) are reported (Li and Zheng, 1982). The upper part has a thickness of ~70 m, consisting of poorly sorted gray pebble and cobble conglomerates (generally 10–30 cm in diameter, with the largest being more than 1 m), with associated semi-solid sandstones and siltstone layers. The conglomerate is very poorly sorted, and the pebble and cobble is always angular or sharp. In the Suerkuli Basin (Fig. 2b) and northern margin of Qaidam Basin (Sun et al., 2005a,b), the Pliocene Shizigou Formation is capped, with an angular unconformity relationship, by the Pleistocene sediments of the Qigequan Formation which consists of poorly sorted conglomerates as well.

3. Methodology

In this study, we collected 150 block samples in the Daban section from the siltstone or sandstone layers. The sampling interval usually varied between 2 and 5 m, depending on the lithology. The block samples were oriented by magnetic compass in the field. For paleomagnetic analysis, cubic specimens of 2.0 cm × 2.0 cm × 2.0 cm were obtained from these block samples in the laboratory.

All the collected oriented specimens were subjected to stepwise thermal demagnetization using a MMTD-60 thermal demagnetizer, and remanence was measured using a 2G Enterprises Model 760-R cryogenic magnetometer installed in a magnetically shielded space (<300 nT) at the Institute of Geology and Geophysics, Chinese Academy of Sciences. Samples were heated up to a maximum temperature of 680 °C with 20–50 °C temperature increments.

Rock magnetic methods include temperature-dependent susceptibility (χ–T) curves and isothermal remanent magnetization (IRM) acquisitions were measured on selected samples. Temperature-dependent susceptibility (χ–T) curves were measured in an argon atmosphere at a frequency of 976 Hz from room temperature up to 700 °C and back to room temperature using a KappaBridge magnetic susceptibility meter (model MFK1-FA) equipped with a CS-3 high-temperature furnace (AGICO Ltd., Brno, Czech Republic). IRM acquisitions were determined using an ASC IM-10-30 pulse magnetizer up to saturation IRM (SIRM) at a maximum applied field of 2.7 T and AGICO JR-6A for remanence measurements.

4. Results

4.1. Magnetic mineralogy

Each of the χ–T heating curves undergoes a marked decrease near 580 °C, which suggests the ubiquitous occurrence of magnetite in the sediments (Fig. 3). χ increases during subsequent cooling after heating to 700 °C. This may result from the neoformation of

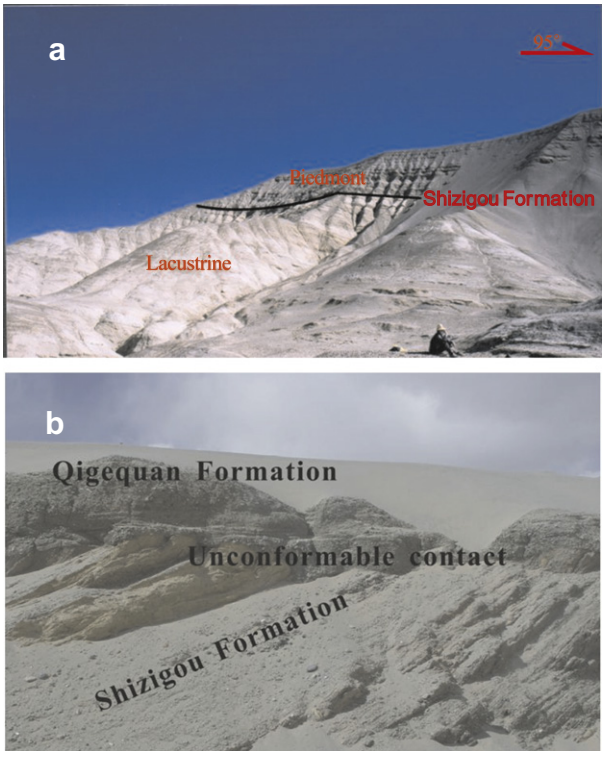

Fig. 2. Field photographs of the Daban section. (a) Depositional facies change in the Daban section from Suerkuli Basin. (b) Angular unconformity between Shizigou Formation and Qigequan Formation in Suerkuli Basin.

fine-grained magnetite via annealing of iron-containing paramagnetic minerals (Ao et al., 2009, 2010). Hematite was usually not obvious in the χ–T curves due to its weak magnetism, however, all the χ–T curves still displayed a decreased χ between ~580 and ~680 °C, suggesting a relatively high concentration of hematite in these samples (Ao et al., 2009). All the IRM acquisition curves indicate that these samples are not saturated even at 2.7 T (Fig. 4), which is consistent with a significant hematite contribution. These results are in agreement with rock magnetic characteristics from previously reported Neogene red beds from the Suerkoli (Xorkoli) basin (Dupont-Nivet and Butler, 2003).

4.2. Magnetostratigraphy

Progressive demagnetization successfully isolated Characteristic Remanent Magnetization (ChRM) components for most of the samples after removing a viscous component of magnetization. Demagnetization results were evaluated using orthogonal diagrams (Zijderveld, 1967) and stereographic projections. ChRM directions were analyzed by principal component analysis (Kirsvink, 1980). Site and group mean directions were calculated using Fisher statistics (Fisher, 1953). For most samples, the high-stability ChRM component was separated between 400 and 680 °C, suggesting that magnetite and hematite are the dominant remanence carrier (Fig. 5a–c). For some samples, a high-stability ChRM component extends to a maximum temperature of 580 °C suggesting magnetite is the dominant remanence carrier (Fig. 5d–f). Specimens not included in our magnetostratigraphic analysis were rejected based on two criteria. (1) ChRM directions could not be determined because of ambiguous or noisy orthogonal demagnetization disgrams. (2) Obtained ChRM directions have maximum angular deviation below 10°. Finally, a total of 127 (75%) samples gave ChRM directions. The strikes and dips of the sediments are similar throughout the section such that the fold test is not significant. After tilt correction, these ChRM directions plot in antipodal normal and reversed orientations on an equal area projection suggesting a primary record of the earth's magnetic field (Fig. 6a). In Fig. 6b, histograms of Cartesian coordinates of means of para-data sets drawn from the data shown in Fig. 6a. In the plots, the reversed polarity directions has been flipped to their antipodes. The intervals containing 95% of each set of components are drawn (see the dashed lines and solid lines). Because the confidence bounds from the two data sets overlap in all three components, the means of the reversed and normal modes cannot be distinguished in at the 95% level of confidence; they pass the bootstrap reversals test (McFadden and McElhinny, 1990; Tauxe, 1998). Normal and reversed directions are all within 45° from the mean normal and reversed directions respectively and are therefore suitable to define the succession of magnetostratigraphic polarity zones (Fig. 6a, b and Table 1). Polarity zones were defined by at least four successive ChRM directions.

The obtained magnetostratigraphic polarity zonation indicates seven normal and seven reversed polarity zones (Fig. 7). To correlate to the revised geomagnetic polarity timescale (GPTS) (Cande and Kent, 1995), the age range is first constrained by the occurrence of Pliocene fossils in the lower lacustrine sequence (Li and

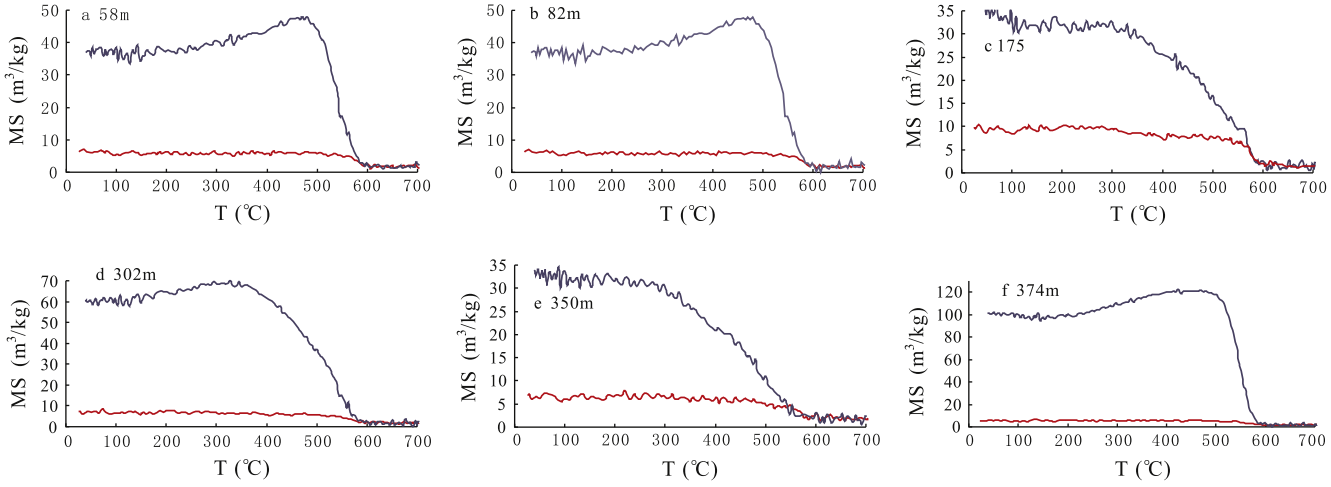

Fig. 3. Magnetic Susceptibility vs. Temperature (χ–T) curves from selected samples of at various meter levels of the Daban section. Heating and cooling cycles are indicated in red and blue respectively. (For interpretation of the references to color in this figure legend, the reader is referred to the web version of this article.)

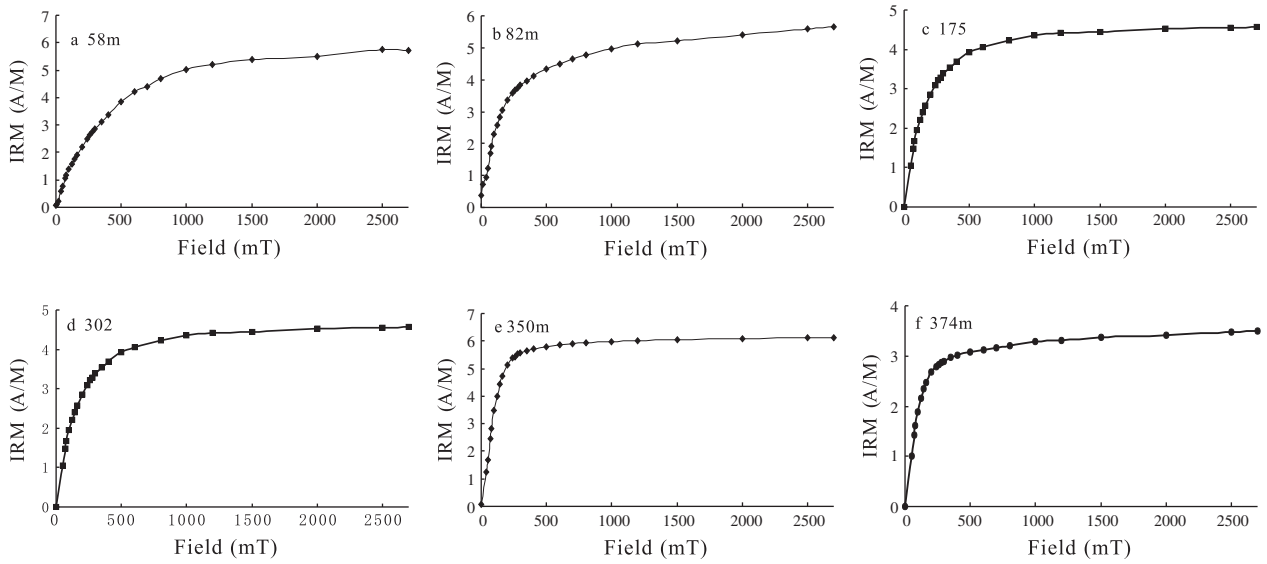

Fig. 4. Isothermal Remanent Magnetization (IRM) acquisition curves for selected samples from the Daban section.

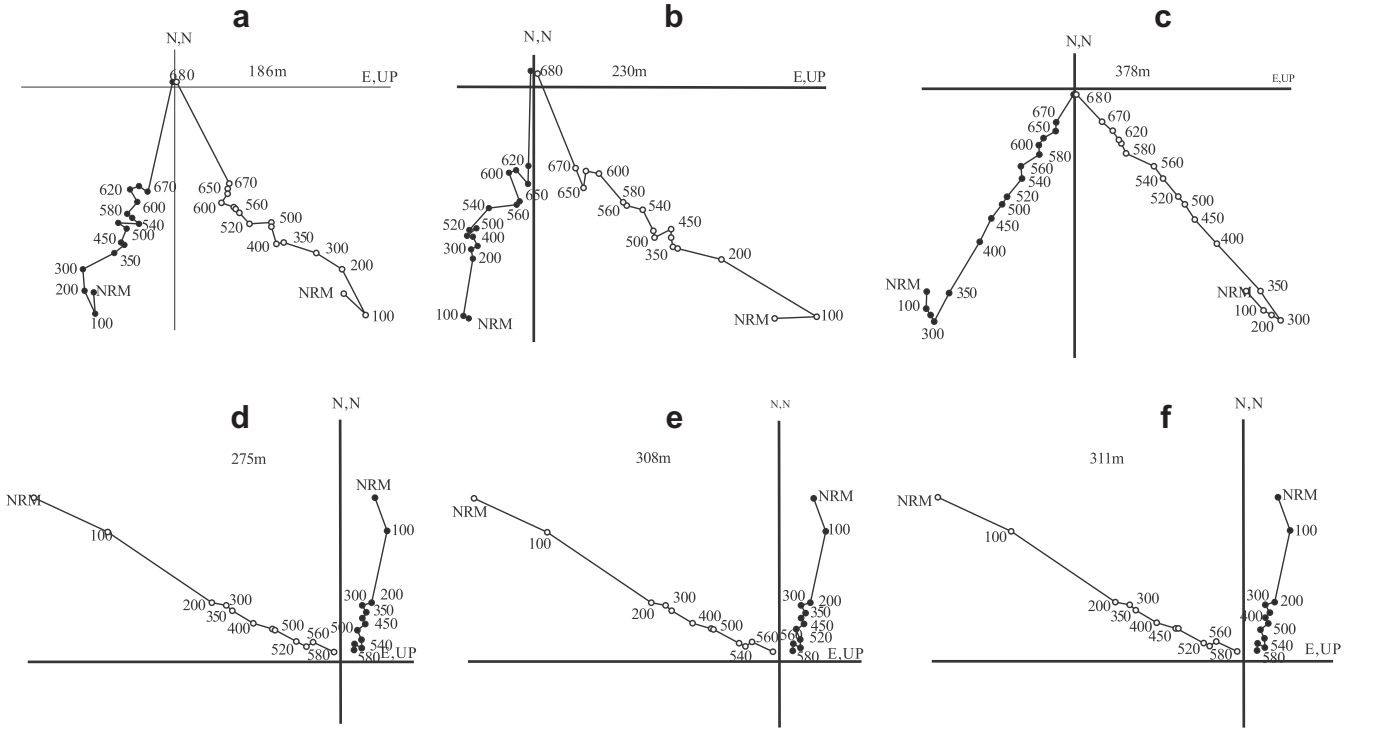

Fig. 5. Orthogonal projections of representative progressive thermal demagnetization for selected samples from the Daban section. The solid and open circles represent the horizontal and vertical planes respectively. The numbers refer to the temperatures in °C. NRM is the natural remanent magnetization.

Zheng, 1982) and the overlying Pleistocene Qigequan Formation. We have not recovered any mammalian fossils within our studied section. However, previous magnetostratigraphic and biostratigraphic studies in the nearby Qaidam Basin suggested that the age of the Shizigou Formation ranges from 8 Ma to 2.6 Ma (Fang et al., 2007). Given the general Pliocene age and the pattern of the polarity zones, an unequivocal correlation is provided by the top of C2An.1n to the top of C3r, covering an age range from ~5.3 to 2.9 Ma (Fig. 7).

4.3. Accumulation rates and facies change at 3.2 Ma

Our rock magnetic analysis indicates a mixture of magnetite and hematite in the sediments from the Suerkuli Basin. There is an abrupt change in depositional conditions at ~3.2 Ma as estimated from our magnetostratigraphic results (Fig. 6). This change corresponds to the marked the transition at the top of the Shizigou Formation (see Geological Setting). This change is associated with a strong increase of sediment accumulation rates from 150 to 215 m/

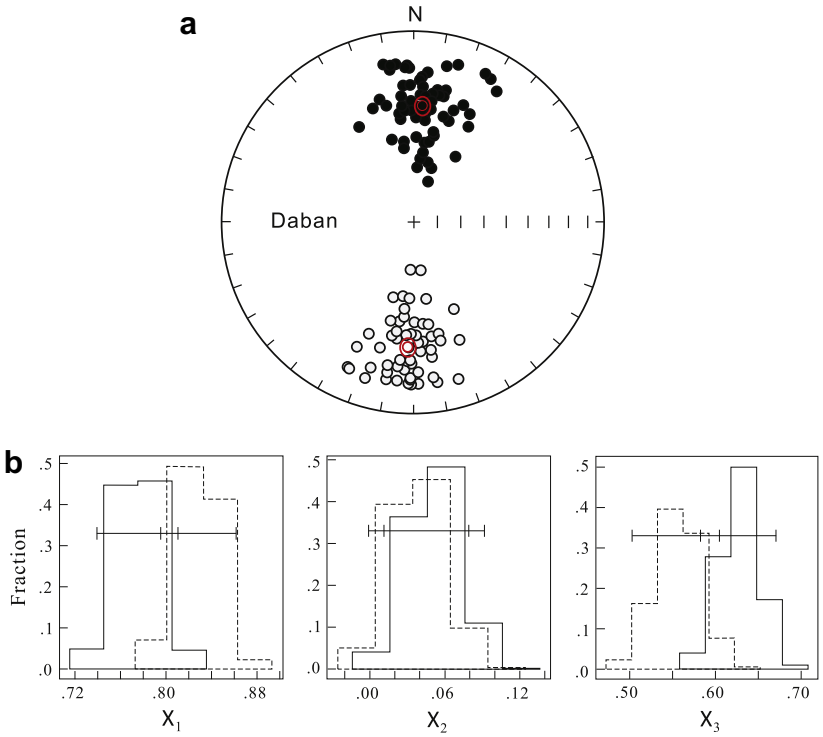

Fig. 6. (a) Equal-area projections of the Characteristic remanent magnetization (ChRM) directions and mean directions (with oval of 95% confidence) for the Daban section. Downward (upward) directions are shown as filled (open) circles. (b) Bootstrap reversal test diagram (Tauxe, 1998). Reversed polarity directions have been inverted to their antipodes to test for a common mean for the normal and reversed magnetization directions. The 95% confidence intervals for all components overlap, indicating a positive reversal test.

Table 1
Paleomagnetic data from the Daban magnetostratigraphic section in Suerkuli Basin.

Shizigou Formation	*N*/*n*	Tilt corrected				
		Dec (°)	Inc (°)	α_{95}	Lat (°)	Long (°)
Normal polarities	150/71	1.82	45.83	4.16	78.6	262.67
Reversed polarities	150/56	183.3	−42.96	5.87	−76.15	78.3
Combined	150/127	2.47	44.5	5.32	77.46	260.63

N is the total number of samples collected and *n* is the number of samples used in the calculation of a (normal, reversed, or combined) mean direction. Abbreviations: Dec, declination; Inc, inclination; α_{95}, statistical parameter associated with means; Lat and Long are east-longitude of the paleomagnetic pole positions.

Ma. Deposits between 5.3 and 3.2 Ma with relatively lower accumulation rates are dominated by mudstones with horizontal beddings, mostly representing lacustrine environment with typical distal source regions. In contrast, after 3.2 Ma deposits with relatively higher accumulation rates are dominated by coarse conglomerates, representing typical proximal fan facies.

5. Discussion

Several lines of evidence suggests that this change in depositional system may be linked to tectonic activity of the middle ATF. Firstly, the Daban section is now located at the top of southern range of Altyn Tagh with tilted Pliocene succession but horizontal Quaternary succession (Figs. 1b and 2a), strongly suggesting Pliocene tectonism and uplift associated with the ATF activity. During the low accumulation rate period from 5.3 to 3.2 Ma, the Suerkuli Basin likely had a stable low relief, which gave rise to the development of the Suerkuli paleolake and weak physical denudation in the catchments, resulting in the deposition of fine-grained lacustrine mudstones. Starting from ca. 3.2 Ma, strong erosion of the bedrocks lead to coarse clastic particles transported into the basin by high-energy river floods or river systems, resulting in the deposition of thick coarse conglomerates associated with increased sedimentation rate. Our preferred interpretation is that these high energy deposits indicate that the bedrocks were gradually uplifted and tilted by tectonic processes, which gave rise to a high relief in the Suerkuli and drying of the paleolake. This is substantiated by the angular unconformity between Pliocene and Pleistocene in the basin and northern margin of the Qaidam Basin (Sun et al., 2005a,b, 2006) strongly suggesting continuing activity of the ATF during the late Pliocene epoch and into the Quaternary period, since angular unconformity between sediments is remarkable evidence of tectonic movement (Tarbuck and Lutgens, 1993). In addition, Pliocene tectonism and uplift occurring along the ATF is documented by numerous independent evidences from previous studies indicating that a large part of the northern Tibetan Plateau has been deformed and uplifted during the Pliocene (Li et al., 1997; Métivier et al., 1998; Meyer et al., 1998; Zheng et al., 2000; Tapponnier et al., 2001; Fang et al., 2005a,b; Sun et al., 2005a,b; Sun and Liu, 2006).

Although the Late-Pliocene deformation and uplift of the ATF is our preferred candidate for this depositional shift, we cannot rule out that the coeval climatic changes of the global Pliocene Climate Deterioration may have contributed this shift as well (Larsen et al., 1994; Thiede et al., 1998; Kleiven et al., 2002). Associated to this climate change with increased seasonality, it has been previously suggested that the development of glacial and periglacial erosion in Northern Hemisphere and especially in the mountains of the Tibetan Plateau is expected to lead to coarse-grained sedimentation and relatively high sediment accumulation rates as well (Zhang et al., 2001).

6. Conclusions

(1) A detailed magnetostratigraphic study was conducted on a Pliocene sedimentary succession in the Suerkuli Basin along the middle ATF.

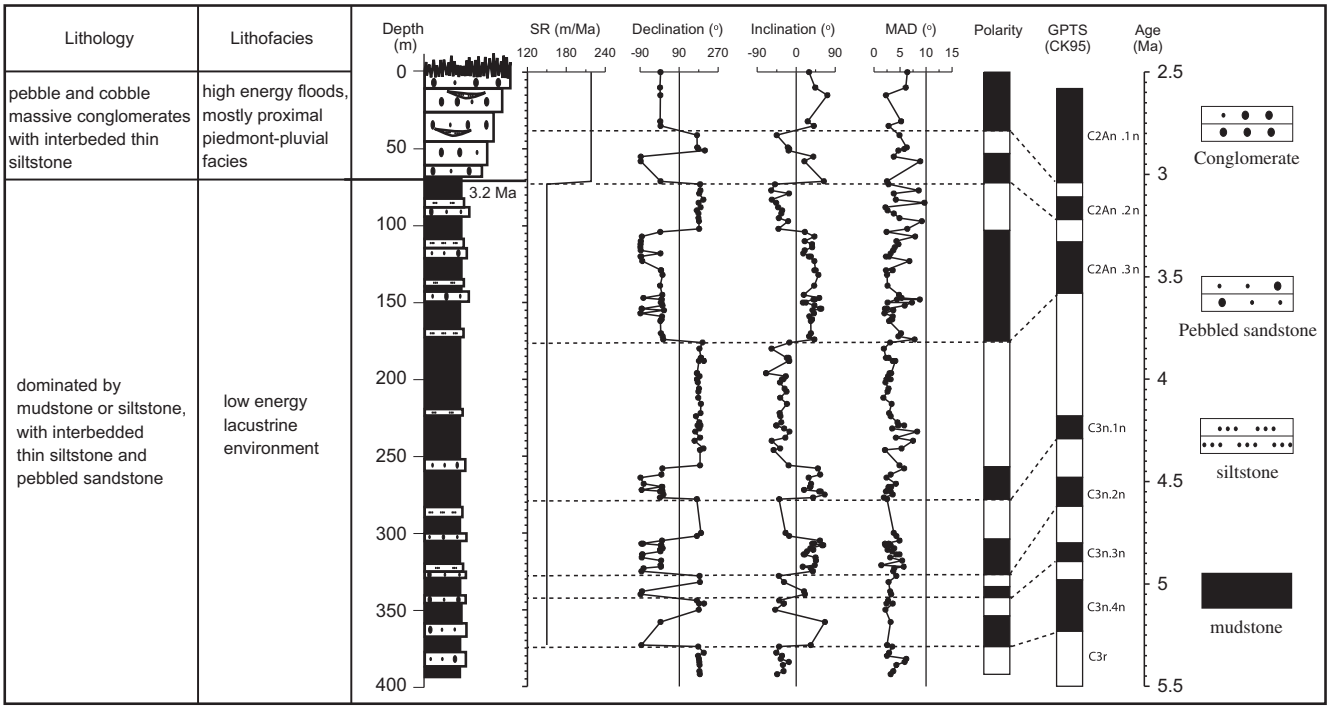

Fig. 7. Lithology, sedimentary facies, sediment accumulation rate, determined magnetostratigraphy of the Daban section, and correlation with geomagnetic polarity timescale (Cande and Kent, 1995). Note the remarkable increase in sediment accumulation rate above the depth of ~70 m and matching with the changes in lithology and sedimentary facies.

(2) This study indicates a strong increase in accumulation rate at ca. 3.2 Ma, associated with a shift in depositional environment from lacustrine to alluvial fan in the Suerkuli Basin.
(3) This shift in depositional environment was possibly linked to deformation and uplift along the ATF although a global climate contribution cannot be ruled out.

Acknowledgements

This study was co-supported by the National Basic Research Program of China (No. 2010CB833400), the Project of the light of the west from the Chinese Academy of Sciences (2008YB01) and the National Natural Science Foundation of China (Nos. 40972123, 40921120406). We are greatful to professor Peter Molnar for his comments and for improving the English. We thank Guillaume Dupont-Nivet, Yin An and two anonymous reviewers for their comments, which significantly improved this paper.

References

Ao, H., Dekkers, M.J., Deng, C.L., Zhu, R.X., 2009. Paleoclimatic significance of the Xiantai fluvio-lacustrine sequence in the Nihewan Basin (North China), based on rock magnetic properties and clay mineralogy. Geophysical Journal International 177, 913–924.

Ao, H., Deng, C.L., Dekkers, M.J., Liu, Q.S., 2010. Magnetic mineral dissolution in the Pleistocene fluvio-lacustrine sediments, Nihewan Basin (North China). Earth and Planetary Science Letters 292, 191–200.

Avouac, J.P., Tapponnier, P., 1993. Kinamatic model of mactive deformation in central Asia. Geophysical Research Letters 20, 895–898.

Cande, S.C., Kent, D.V., 1995. Revised calibration of the geomagnetic polarity timescale for the Late Cretaceous and Cenozoic. Journal of Geophysical Research 100, 6093–6095.

Dupont-Nivet, G., Butler, R.F., 2003. Paleomagnetism indicates no Neogene vertical axis rotations of the northeastern Tibetan Plateau. Journal of Geophysical Research 108, 2386. doi:10.1029/2003JB002399.

Dupont-Nivet, G., Robinson, D., Butler, R., 2004. Concentration of crustal displacement along a weak Altyn Tagh fault: evidence from paleo-magnetism of the northern Tibetan Plateau. Tectonics 23, TC1020. doi:10.1029/2002TC001397.

Fang, X.M., Yan, M.D., Van der Voo, R., Rea, D.K., Song, C.H., Pares, J.M., Gao, J.P., Nie, J.S., Dai, S., 2005a. Late Cenozoic deformation and uplift of the NE Tibetan plateau: evidence from high-resolution magneto stratigraphy of the Guide Basin, Qinghai Province, China. Geological Society of America Bulletin 117, 1208–1225.

Fang, X.M., Zhao, Z.J., Li, J.J., Yan, M.D., Pan, B.T., Song, C.H., Dai, S., 2005b. Magnetostratigraphy of the late Cenozoic Laojunmiao anticline in the northern Qilian Mountains and its implications for the northern Tibetan Plateau uplift. Science of China Series D – Earth Science 48, 1040–1051.

Fang, X.M., Zhang, W.L., Meng, Q.Q., Gao, J.P., Wang, X.M., King, J., Song, C.H., Dai, S., Miao, Y.F., 2007. High-resolution magnetostratigraphy of the Neogene Huaitoutala section in the eastern Qaidam Basin on the NE Tibetan Plateau, Qinghsi Province, China and its implication on tectonic uplift of the NE Tibetan Plateau. Earth and Planetary Science Letters 258, 293–306.

Fisher, R.S., 1953, Dispersion on a sphere. Proceedings of Royal Society, vol. 217 (Ser.A), pp. 295–302.

Kirsvink, J.L., 1980. The least squares line and plane and the analysis of paleomagnetic data. Geophysics Journal of the Royal Astronomical Society 62, 699–712.

Kleiven, H.F., Jansen, E., Fronval, T., Smith, T.M., 2002. Intensification of Northern Hemisphere glaciations in the circum Atlantic region (3.5–2.4 Ma) ice-rafted detritus evidence. Palaeogeography Palaeoclimatology Palaeoecology 184, 213–223.

Larsen, H.C., Saunders, A.D., Clift, P.D., Beget, J., Wei, W., Spezzaferri, S., 1994. ODP Leg 152 Scientific Party, Seven million years of glaciation in Greenland. Science 264, 952–955.

Li, T.D., Zheng, S.J., 1982. The tertiary in the middle of the Altyn Tagh, Xinjiang, China. Northwest Geology 15, 1–11 (in Chinese).

Li, J.J., Fang, X.M., Van der Voo, R., Zhu, J.J., Mac Niocaill, C., Cao, J.X., Zhong, W., Chen, H.L., Wang, J.L., Wang, J.M., Zhang, Y.C., 1997. Late Cenozoic magnetostratigraphy (11–0 Ma) of the Dongshanding and Wangjiashan sections in the Longzhong Basin, western China. Geologie en Mijnbouw 76, 121–134.

Li, H.B., Yang, J.S., Shi, R.D., Wu, C.L., Tapponnier, P., Wan, Y.S., Zhang, J.X., Meng, F.C., 2002. Determination of the Altyn Tagh strike-slip fault basin and its relationship with mountains. Chinese Science Bulletin 47, 572–577.

McFadden, P.L., McElhinny, M.W., 1990. Classification of the reversals test in palaeomagnetism. Geophysical Journal International 103, 725–729.

Meng, Q.R., Hu, J.M., Yang, F.Z., 2003. Timing and magnitude of displacement on the Altyn Tagh fault: constraints from stratigraphic correlation of adjoining Tarim and Qaidam basins, NW China. Terra Nova 13, 86–91.

Métivier, F., Gaudemer, Y., Tapponnier, P., Meyer, B., 1998. Northeastward growth of the Tibet plateau deduced from balanced reconstruction of two depositional areas: the Qaidam and Hexi Corridor basins, China. Tectonics 17, 823–842.

Meyer, B., Tapponnier, P., Bourjot, L., Métivier, F., Gaudemer, Y., Peltzer, G., Guo, S.-M., Chen, Z.-T., 1998. Crustal thickening in Gansu-Qinghai, lithospheric mantle

subduction, and oblique, strike-slip controlled growth of the Tibetan Plateau. Geophysical Journal International 135, 1–47.
Rowley, D.B., Currie, B.S., 2006. Palaeo-altimetry of the late Eocene to Miocene Lunpola basin, central Tibet. Nature 439, 677–681.
Sun, J.M., Liu, T.S., 2006. The age of the Taklimakan Desert. Science 312, 1621.
Sun, J.M., Zhu, R.X., An, Z.S., 2005a. Tectonic uplift in the northern Tibetan Plateau since 13.7 Ma ago inferred from molasse deposits along the Altyn Tagh Fault. Earth and Planetary Science Letters 235, 641–653.
Sun, Z.M., Yang, Z.Y., Pei, J.L., Ge, X.H., Wang, X.S., Yang, T.S., Li, W.M., Yuan, S.H., 2005b. Magnetostratigraphy of Paleogene sediments from northern Qaidam Basin, China: implications for tectonic uplift and block rotation in northern Tibetan Plateau. Earth and Planetary Science Letters 237, 635–646.
Sun, Z.C., Qiao, Z.Z., Jing, M.C., Zhang, H.Q., Sun, N.D., Lu, Y.L., Wang, H.J., 2006. Qigequan formation and quaternary-Neogene boundary in Qaidam basin. Oil & Gas Geology 27, 422–432 (in Chinese).
Tapponnier, P., Xu, Z.Q., Roger, F., Meyer, B., Arnaud, N., Wittlinger, G., Yang, J.S., 2001. Oblique stepwise rise and growth of the Tibet Plateau. Science 294, 1671–1677.
Tarbuck, E.J., Lutgens, F.K., 1993. The earth-Fourth Edition. Macmillan Publishing Company, New York, pp. 185–186.
Tauxe, L., 1998. Paleomagnetic Principles and Practice. Kluwer Academic Publishers, Dordrecht, 299.
Thiede, J., Winkler, A., Wolf-Welling, T., Eldholm, O., Myhre, A.M., Baumann, K.H., Henrich, R., Stein, R., 1998. Late Cenozoic history of the polar North Atlantic: results from ocean drilling. Quaternary Science Review 17, 185–208.
Washburn, Z., Arrowsmith, J.R., Dupont-Nivet, G., Feng, X.F., Zhang, Y., Chen, Z., 2004. Paleoseismology of the Xorkol segment of the central Altyn Tagh Fault, Xinjiang, China. Annals of Geophysics 45 (5), 1015–1034.
Yin, A., Rumelhart, P.E., Butler, R., Cowgill, E., Harrison, T.M., Foster, D.A., Ingersoll, R.V., Zhang, Q., Zhou, X.Q., Wang, X.F., Hanson, A., Raza, A., 2002. Tectonic history of the Altyn Tagh Fault system in northern Tibet inferred from Cenozoic sedimentation. Geological Society of America Bulletin 114, 1257–1295.
Yue, Y.J., Ritts, B.D., Graham, S.A., Wooden, J.L., Gehrels, G.E., Zhang, Z.C., 2003. Slowing extrusion tectonics: lowered estimate of post-Early Miocene slip rate for the Altyn Tagh fault. Earth and Planetary Science Letters 217, 111–122.
Zhang, P.Z., Molnar, P., Downs, W.R., 2001. Increased sedimentation rates and grain sizes 2–4 Myr ago due to the influence of climate change on erosion rates. Nature 410, 891–897.
Zhang, P.Z., Sheng, Z.K., Wang, M., Gan, W.J., Bürgmann, R., Molnar, P., Wang, Q., Niu, Z.J., Sun, Z.Z., Wu, J.C., Sun, H.R., You, X.Z., 2004. Continuous deformation of the Tibetan Plateau from global positioning system data. Geology 32, 809–812.
Zheng, H.B., Powell, C.M., An, Z.S., Zhou, J., Dong, G.R., 2000. Pliocene uplift of the northern Tibetan Plateau. Geology 28, 715–718.
Zijderveld, J.D.A., 1967. AC demagnetization of rocks: analysis of results. In: Collision, D.W., Creer, K.M., Runcorn, S.K. (Eds.), Methods in Paleomagnetism. Elsevier, pp. 254–286.